Solar and Atmospheric Neutrinos in Super-Kamiokande

J.L. Raaf, on behalf of the Super-Kamiokande Collaboration
Boston University Physics Department, Boston, MA 02215, USA
E-mail: jlraaf@icrr.u-tokyo.ac.jp

Abstract. The Super-Kamiokande (SK) water Cherenkov detector has been operating for nearly 12 years collecting data for the study of both solar and atmospheric neutrinos as well as searching for neutrinos from supernovæ(and relic supernovæ) and for nucleon decay. The experiment has undergone three operating phases during the full running period: SK-I (40% photocathode coverage), SK-II (20% coverage), and SK-III (40% coverage). Soon, the experiment will move into its fourth phase when the data acquisition electronics are upgraded in late 2008. Presented here are neutrino oscillation results from SK-I and SK-II solar and atmospheric data, and a preliminary look at data from SK-III. Also discussed briefly is the upcoming electronics upgrade that will carry the experiment into its fourth phase.

1. Introduction

Super-Kamiokande [1, 2] is a 50,000 ton (22,500 ton fiducial) water Cherenkov detector located 1000 m underground at the Kamioka Observatory of the Institute for Cosmic Ray Research, University of Tokyo. The detector is cylindrical: 42 m high and 39.3 m in diameter. Neutrino interactions in the water are viewed by $\sim 11,000$ 50-cm photomultiplier tubes (PMTs) facing inward and distributed evenly on the entire inner detector (ID) surface to give 40% photocathode coverage. The inner volume is surrounded by an outer detector (OD) which is instrumented with ~ 1900 smaller 20-cm PMTs facing outward to aid in identification and rejection of cosmic ray events and events arising from interactions that took place in the rock surrounding the detector.

A broad range of energies is studied with the SK detector, from a few MeV up to $\mathcal{O}$(TeV). In the low energy region below ~ 20 MeV, solar neutrino interactions are detected by neutrino-electron scattering. At higher energies, atmospheric neutrino interactions covering 5 orders of magnitude are detectable by neutral- and charged-current neutrino-nucleon scattering.

The Super-Kamiokande running periods are divided into three parts. SK-I ran from 1996 until November 2001, when an accident destroyed more than half of the PMTs. The detector was rebuilt with half the PMT density (and therefore half the photocathode coverage) and resumed data-taking for its second phase from 2003 through October 2005. Restoration of the full 40% photocathode coverage was completed by mid-2006; the SK-III phase has been collecting data since July 2006.

1.1. SK-IV Data Acquisition

In August 2008, the third running period will end in order to upgrade the data acquisition (DAQ) electronics. The upgraded electronics will simplify detector operations by unifying the

readout scheme for the inner and outer detectors (previously distinct). In addition, we expect both increased reliability (due to fewer discrete components) and increased performance (in the form of improved energy resolution, improved multiple-hit capability, lower single photo-electron hit thresholds, and improved supernova burst capability). The ethernet-based readout will allow for increased bandwidth and reduced deadtime.

In the DAQ system employed for SK-I, -II, and -III, a hardware trigger (issued when the number of PMT hits in a 200 ns timing window exceeds a threshold) is utilized to reduce the amount of data sent from the readout modules to the front-end DAQ computers. In the SK-IV DAQ, no hardware trigger will be used. Instead, all PMT hits will be sent to the front-end computer by a periodic timing signal and software triggers will be applied to select interesting event windows. This new scheme is a novel approach to data acquisition for Super-K; it provides much greater flexibility in triggering than the previous DAQ system allowed.

2. Solar Neutrinos

At low energies, Super-Kamiokande is sensitive primarily to neutrinos from the ^8B branch of the pp nuclear fusion chain in the Sun. The neutrinos produced in this branch range in energy from less than 1 MeV to near 20 MeV. Another small contribution to the solar neutrino flux at SK is that of *hep* neutrinos, which may be observable at the high end of the solar neutrino range because their endpoint is slightly above the endpoint of ^8B neutrinos.

At energies below $\sim$ 5 MeV, radioactive backgrounds dominate, making it very difficult to select solar neutrino events. Above that threshold, events are detectable in SK by Cherenkov light from a recoiling atomic electron in a $\nu - e^-$ scatter. The energy of the recoil electron and its direction relative to the Sun are reconstructed; electrons that were scattered by neutrinos point in a direction that is correlated with the Sun. This is demonstrated with 289 days of SK-III data in Fig. 1.

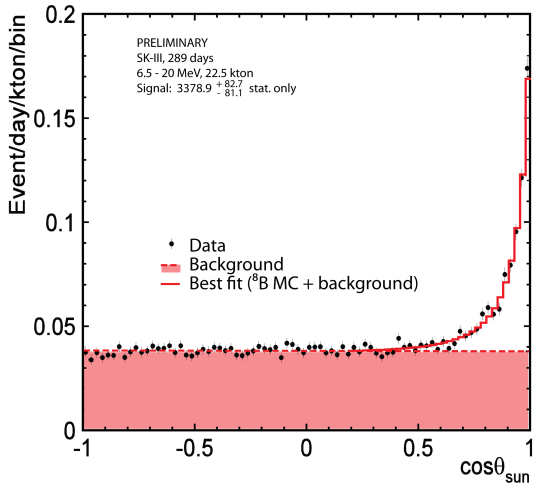

Figure 1. Preliminary fit to angular distribution of solar neutrino event candidates for 289 days of SK-III data. The elastic scattering peak is indicated by the solid red line, the background by the shaded region.

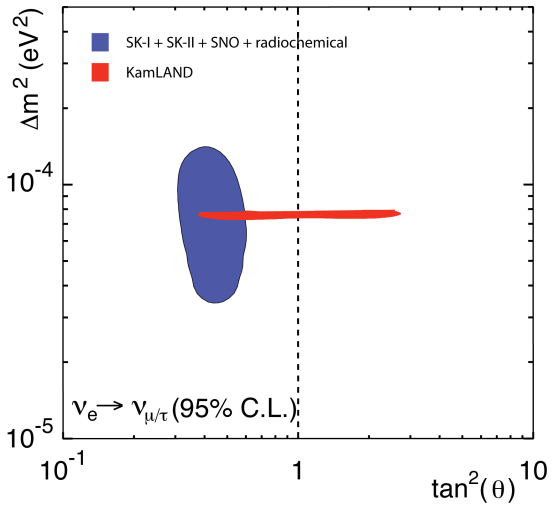

Figure 2. Allowed oscillation parameter region obtained from a combined fit to experimental data from SK-I, SK-II, SNO [3, 4], Homestake [5], SAGE [6], and GALLEX/GNO [7] shown in blue. Overlaid in red is the KamLAND [8] allowed region.

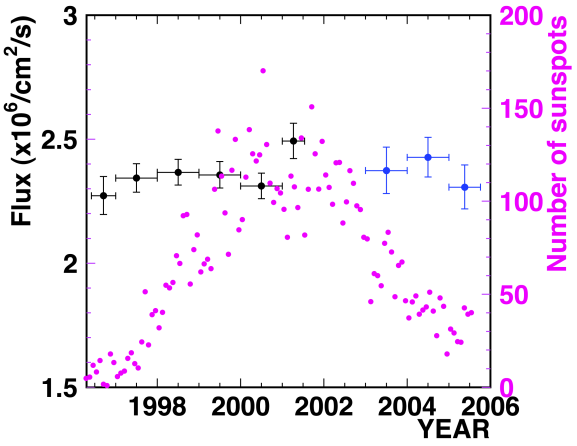

Figure 3. SK-I (black dots) and SK-II (blue dots) solar neutrino flux compared to sunspot activity (pink dots) during the periods of SK-I and SK-II data-taking. No correlation with solar cycle minima or maximum is seen.

The original goal of the SK solar neutrino measurement was to look for flux-independent evidence of neutrino oscillations such as a difference of daytime and nighttime fluxes, seasonal variations of the flux, and/or spectrum distortion. Although no significant evidence for any of these has been observed, the non-observation has allowed Super-Kamiokande to help place a strong constraint on the solar neutrino oscillation parameters. Fig. 2 shows the 95% C.L. allowed region of oscillation parameter space for a combined fit to experimental data from SK-I, SK-II, SNO, and radiochemical experiments. Also shown is the KamLAND allowed region which strongly constrains the mass difference.

Because the SK-I and SK-II solar neutrino datasets span an interval of 9.5 years coinciding with nearly the full period of solar cycle 23, it is also interesting to check for correlation of the measured solar neutrino flux with the number of sunspots. The SK-I and -II data are compiled into 1-year bins between 1996 and 2006 and the fluxes for these years are shown along with the solar activity in Fig. 3. The solar neutrino flux is stable across this time period and shows no correlation with the minima and maximum of solar cycle 23.

3. Atmospheric Neutrinos

Atmospheric neutrinos span a much wider range of energies than solar neutrinos, and their pathlength plays an important role in the observation of oscillations. The incoming direction of a neutrino specifies the distance travelled from production source to the detector. The range of pathlengths is from 10 km to 13,000 km; the energies span 5 orders of magnitude.

Because of the broad scope these events, atmospheric neutrino interactions are divided into categories. Fully contained (FC) events have their interaction vertex inside the fiducial volume of the detector and all produced particles stop within the inner detector. Partially contained (PC) event vertices are also required to be within the fiducial volume, but in this case some of the produced particle tracks escape to the outer detector. The average neutrino energy is ~ 1 GeV for FC and ~ 10 GeV for PC events. FC events are further divided into sub-categories based on their visible energy: sub-GeV ($E_{\rm vis} < 1.33$ GeV), and multi-GeV ($E_{\rm vis} > 1.33$ GeV). The other broad category of atmospheric neutrino events is upward-going muons, which are created by neutrino interactions in the rock beneath the SK detector. They either stop inside the detector ("upward stopping") or pass through the detector entirely ("upward through-going"). The average parent neutrino energies for these events are ~ 10 GeV and ~ 100 GeV, respectively.

The two flagship oscillation analyses for SK atmospheric neutrinos are the fine-binned zenith angle 2-flavor analysis [9] and the "L over E" (L/E) analysis [10]. The zenith angle analysis looks for a distortion of the zenith angle spectrum in many sub-samples of data. The L/E analysis uses a much more selective subsample of data, requiring only events with good resolution of L/E, and looks for an expected sinusoidal pattern of oscillatory behavior.

Recently the SK-I and SK-II full datasets were re-analyzed after improvements to both the Monte Carlo simulation and the event reconstruction algorithms. Some of the changes to the simulation include: an update of the atmospheric neutrino flux model to the so-called "Honda 06" model [11]; various modifications to the neutrino interaction model [12], (*e.g.*, change of quasi-elastic and single pion axial mass to $M_A = 1.2$ GeV, addition of lepton mass effects for charged-current single pion production, and addition of the pion-less delta decay channel $\Delta \rightarrow N\gamma$); improvements to the detector simulation model of light reflections and scattering; better tuning of outer detector parameters in the simulation; and improvements in the ring counting algorithm. Additionally, at the time of re-analysis, the systematic uncertainties were re-evaluated and a few new uncertainties were added.

The re-analysis of SK-I and SK-II data are presented here for the 2-flavor zenith angle analysis and for the L/E analysis.

3.1. 2-flavor zenith angle analysis

In the zenith angle analysis, data are binned according to event type (FC/PC/upward-going muon, μ-like or electron-like, number of rings), energy, and zenith angle, leading to a total of 400 bins for SK-I data, and 350 bins for SK-II data. Because of lower statistics, the energy-binning for SK-II is adjusted relative to SK-I to avoid effects from bins with too few events. A χ^2 fit in bins of zenith angle is done with 90 systematic error pull terms to account for uncertainties in neutrino flux, cross sections, event reconstruction, and data reduction. The results of the combined SK-I and SK-II fit are shown in Fig. 4 overlaid with 1489 days of SK-I data. The minimum $\chi^2 = 832.8$ (745 d.o.f.) is located at $\Delta m^2 = 2.1 \times 10^{-3}$ eV^2 and $\sin^2 2\theta = 1.02$. The χ^2 value obtained for a no-oscillation hypothesis is 1395.6 for 747 d.o.f.

3.2. L/E analysis

In the L/E analysis, a good resolution for neutrino flight pathlength, L, and energy, E, are necessary when trying to observe the expected dip in the spectrum due to oscillations. Strict selection criteria are applied to events for this analysis because events with poor pathlength and energy resolution would smear the distribution and cause the dip to be washed out. A χ^2 fit to 43 bins of $\log_{10}(L/E)$ is done for SK-I and SK-II data with 29 systematic uncertainty pull terms. The minimum $\chi^2 = 78.9$ (83 d.o.f.) is located at $\Delta m^2 = 2.2 \times 10^{-3}$ eV^2 and $\sin^2 2\theta = 1.04$. The data exclude the other hypotheses at 4.1σ for neutrino decay [13] and 5.0σ for decoherence [14]. A plot of the L/E distribution after selection cuts and strict cuts on the L/E resolution is shown in Fig. 5 with the best fits to oscillations, neutrino decay, and neutrino decoherence. The first dip is clearly visible in the region around 500 km/GeV and cannot be explained the other two hypotheses shown in the figure.

The allowed region at 90% C.L. is consistent with the results from the 2-flavor zenith angle analysis but gives a tighter range of allowed Δm^2. The results of both analyses are shown together in Fig. 6.

4. The Future of Super-Kamiokande

Analysis of the SK-III dataset is underway for both solar and atmospheric neutrinos. A preliminary comparison of these data with SK-I and SK-II distributions shows agreement for both.

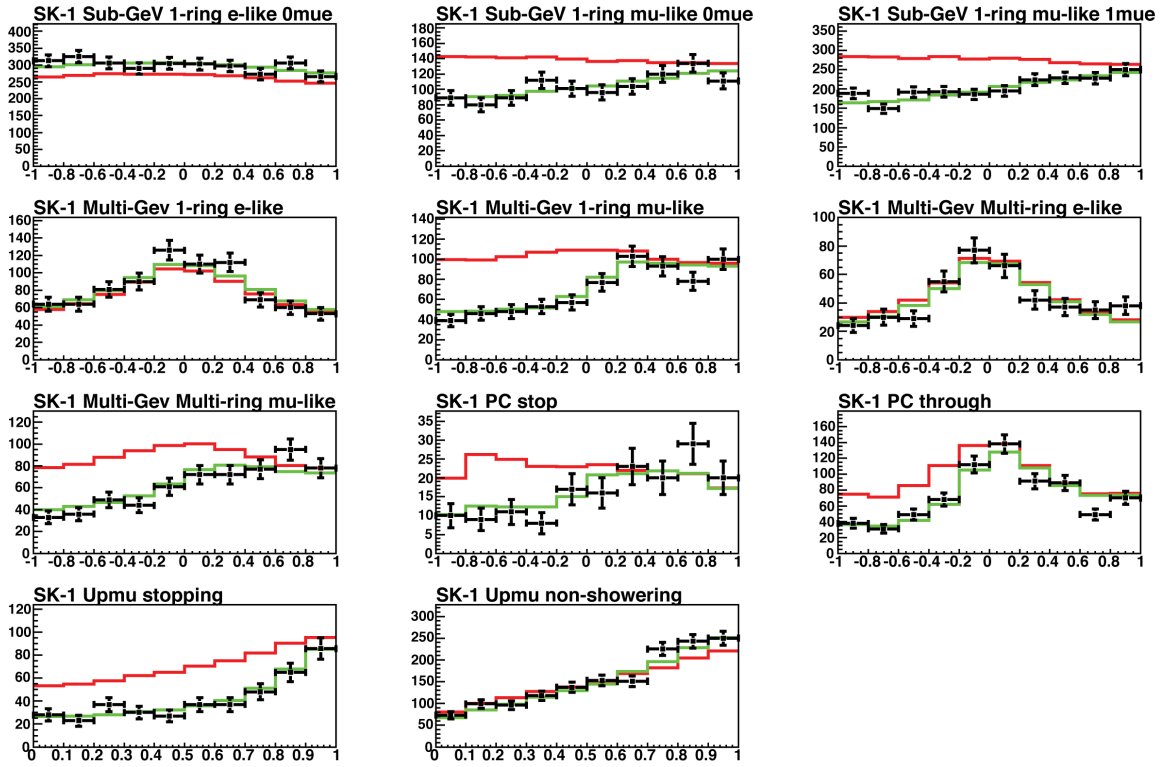

Figure 4. Zenith angle distributions for the 2-flavor fine-binned analysis. Data are indicated by black dots, un-oscillated Monte Carlo by the red solid line, and the best fit to 2-flavor oscillations by the solid green line.

4.1. Solar neutrinos

In addition to finishing the standard analysis for SK-III, work is being done to observe other predicted effects for solar neutrino oscillations. One yet-to-be-observed prediction for the LMA solution to solar neutrino oscillations is the upturn of the energy spectrum at low energy; observation of this is a main goal of the future solar neutrino program at Super-K, where the effect could be as large as 10% at 4 MeV. Although the current energy threshold is 5 MeV, the collaboration is working hard to further reduce backgrounds at low energy in order to achieve a 4 MeV threshold.

4.2. Atmospheric neutrinos

Analysis of the combined SK-I, -II, and -III atmospheric neutrino datasets will not only increase the precision of the "Standard Model" parameter measurements Super-Kamiokande has already made, but also allow for analyses of more subtle effects. These high-statistics datasets make it feasible to search for sub-dominant, exotic, and non-oscillation physics as well. Many of these scenarios have already been investigated using Super-Kamiokande data, or are currently under study.

Acknowledgments

The author and the Super-Kamiokande collaboration gratefully acknowledge the cooperation of the Kamioka Mining and Smelting Company. The Super-Kamiokande experiment has been built and operated from funding by the Japanese Ministry of Education, Culture, Sports, Science and

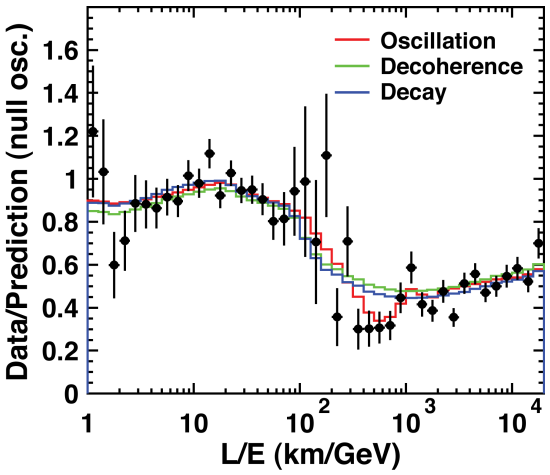

Figure 5. L/E distributions for the combined SK-I and SK-II datasets. Data are indicated by black dots and the best fit to oscillations is shown by the red line. Two other hypotheses, neutrino decay and neutrino decoherence, are indicated by the blue and green lines, respectively.

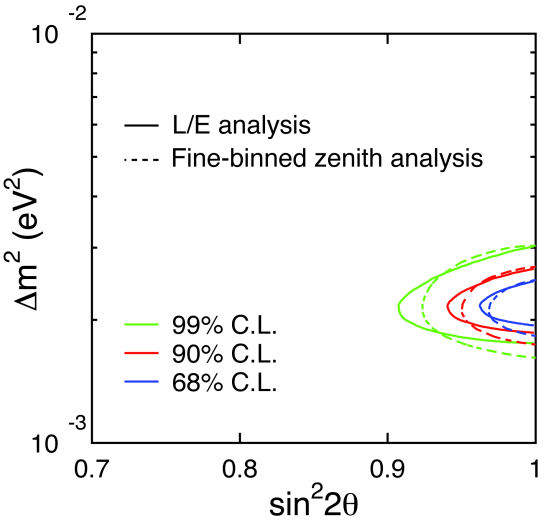

Figure 6. Allowed parameter regions for the L/E analysis (solid lines) and the 2-flavor fine-binned zenith angle analysis (dashed lines).

Technology, the United States Department of Energy, and the U.S. National Science Foundation.

References

[1] Super-Kamiokande Collaboration URL `http://www-sk.icrr.u-tokyo.ac.jp/sk/about/col_sk-e.html`

[2] Fukuda S *et al.* (Super-Kamiokande) 2003 *Nucl. Instrum. Methods* **A501** 418

[3] Ahmad Q R *et al.* (SNO) 2002 *Phys. Rev. Lett.* **89** 011302 (*Preprint* `nucl-ex/0204009`)

[4] Aharmim B *et al.* (SNO) 2005 *Phys. Rev.* **C72** 055502 (*Preprint* `nucl-ex/0502021`)

[5] Cleveland B T *et al.* 1998 *Astrophys. J.* **496** 505–526

[6] Abdurashitov J N *et al.* (SAGE) 1999 *Phys. Rev.* **C60** 055801 (*Preprint* `astro-ph/9907113`)

[7] Altmann M *et al.* (GNO) 2000 *Phys. Lett.* **B490** 16–26 (*Preprint* `hep-ex/0006034`)

[8] Abe S *et al.* (KamLAND) 2008 *Phys. Rev. Lett.* **100** 221803 (*Preprint* `0801.4589`)

[9] Ashie Y *et al.* (Super-Kamiokande) 2005 *Phys. Rev.* **D71** 112005 (*Preprint* `hep-ex/0501064`)

[10] Ashie Y *et al.* (Super-Kamiokande) 2004 *Phys. Rev. Lett.* **93** 101801 (*Preprint* `hep-ex/0404034`)

[11] Honda M, Kajita T, Kasahara K, Midorikawa S and Sanuki T 2007 *Phys. Rev.* **D75** 043006 (*Preprint* `astro-ph/0611418`)

[12] Hayato Y 2002 *Nuclear Physics B Proceedings Supplements* **112** 171–176

[13] Barger V D *et al.* 1999 *Phys. Lett.* **B462** 109–114 (*Preprint* `hep-ph/9907421`)

[14] Lisi E, Marrone A and Montanino D 2000 *Phys. Rev. Lett.* **85** 1166–1169 (*Preprint* `hep-ph/0002053`)